Sensitivity of a Large-Scale Ocean Model to a Parameterization of Topographic Stress

MICHAEL EBY AND GREG HOLLOWAY

Institute of Ocean Sciences, Sidney, British Columbia, Canada

(Manuscript received 8 June 1993, in final form 2 June 1994)

ABSTRACT

A conventional ocean model was revised to include a tendency for velocities to relax toward a maximum entropy solution that depends on the shape of topography. The tendency, called topographic stress, generates poleward eastern boundary undercurrents, strengthens equatorward deep western boundary currents, sustains a deep Alaska Stream, and contributes to deep water exchange. Although the influence of topographic stress is most clearly seen at depth, surface expressions include reducing the overshoot of western boundary current separation, thereby limiting implied air–sea heat and freshwater fluxes near these separations.

1. Introduction

Eddies interacting with bottom topography can exert large systematic forces (topographic stress) upon the mean circulation. Usual eddy parameterizations in terms of bottom drag or eddy viscosity move a model toward a state of rest, whereas topographic stress may be a driving force behind mean flows. It has been suggested by Holloway (1992) that a more skillful representation of unresolved eddies may be given by the tendency toward higher system entropy.

Salmon et al. (1976) examined statistical dynamical tendencies in the context of ideal quasigeostrophic dynamics. Among their simplest results is the expectation that, on scales larger than the first deformation radius, motion should tend to be barotropic and given by a streamfunction (which we express in terms of transport) satisfying

$$(\alpha/\beta - \nabla^2)\langle\psi\rangle = h, \tag{1}$$

where ∇^2 is the two-dimensional Laplacian, α/β is a ratio of Lagrange multipliers (due to dynamics which conserve energy and enstrophy), $h = f\delta H$ is the depth-integrated potential vorticity due to variation δH about mean depth, and f is the Coriolis parameter. This equation implies that an ocean with no external forcing, filled with random eddies (without mean motion), would tend to set up a mean flow (ψ) that depends on the topography (h).

The idealizations underlying (1) are so extreme that methods of statistical mechanics are often regarded as having no practical oceanographic application. The ocean is manifestly an open system (with external forcing and internal dissipation), based on full physics. Nevertheless, Holloway (1992) suggests that ocean models that cannot adequately resolve eddies are systematically corrupted by the absence of a tendency toward (1). We investigate the effects of modifying a coarse-resolution ocean model such that the model would relax not toward rest but rather toward a solution such as (1). To test the parameterization, we chose to use a well-known primitive equation model—one which already reproduces the ocean circulation with reasonable skill. We seek to discover how sensitive model results are to the suggested parameterization and, if possible, to see where model results become more or less realistic. We hope that this study will help motivate and guide further theoretical investigation.

2. Implementation

For this study we used the GFDL Modular Ocean Model (MOM) (Pacanowski et al. 1991), which is based on code originally formulated by Bryan (1969) and further developed by Semtner (1974) and Cox (1984).

Given a coarse-resolution model, Holloway (1992) suggests a simplified expression for the maximum entropy equilibrium solution as

$$\psi = -fL^2H, \tag{2}$$

where $L = \sqrt{\beta/\alpha}$ is a length scale and H is the total depth. This approximation of the transport streamfunction given by (1) is based on the assumptions that the model grid is more coarse than L and that the length scale for typical variation of H is much smaller than the scale for variation of f.

For practical applications L is difficult to determine since its theoretical motivation depends upon artifacts such as ideal dynamics with finite spectral truncation. Plausibly L is related to eddy length scales (Cummins and Holloway 1994). For the purpose of preliminary

Corresponding author address: Michael Eby, Institute of Ocean Sciences, P.O. Box 6000, Sidney, BC V8L 4B2, Canada.

sensitivity testing, we treat L as an adjustable parameter, presumed to follow eddy length scales in a regionally averaged manner. One could make a simpler choice to take L as a constant of order 10 km. In fact we have previously done so (results not shown). The consequence of constant L is that a choice, which has significance at low latitudes, is overwhelming at higher latitudes. We impose a simple, ad hoc formula $L = 7.5 + 4.5 \times \cos(2 \times \text{lat})$, which causes L to diminish from 12 km near the equator to 3 km near the pole. Clearly this invites parameter tuning. At present, our aim is only to observe sensitivity.

The maximum entropy solution can be written in terms of velocity as

$$u^* = -\frac{1}{H}\frac{\delta\psi}{\delta y}, \quad v^* = \frac{1}{H}\frac{\delta\psi}{\delta x}. \tag{3}$$

By modifying the horizontal viscosity parameterization in the momentum equation, the model solution is forced to relax toward the maximum entropy equilibrium velocities with a no-slip boundary condition. The modified viscous tendencies are

$$A_m\nabla^2(u - u^*), \quad A_m\nabla^2(v - v^*), \tag{4}$$

where A_m is eddy viscosity and u and v are model velocities.

3. Model setup

A global model was created with grid spacing 1.875° in longitude and 1.856° in latitude, which closely approximates a spectral T64 grid. Thirty-one levels were used with layer thicknesses ranging from 50 to 300 m. Topography was extracted from ETOPO5 (1986) using a raised cosine weighted average of the data within a grid cell. Eight islands were included: Madagascar, Australia, New Zealand, Japan, Iceland, and Svalbard plus Antarctica and an artificial island at the North Pole.

The model was forced with annual-mean Hellerman and Rosenstein (1983) wind stress and a 30-day relaxation of surface salinity and temperature to annual mean Levitus (1982) climatology. Fourier filtering was applied to latitudes north of 70°. Horizontal viscosity, horizontal diffusion, vertical viscosity, and vertical diffusion were set to 2×10^5, 2×10^3, 2×10^{-3}, and 1×10^{-4} m^2 s^{-1}, respectively. Velocity time steps were 15 minutes and the tracer time step was 1 day (Bryan 1984).

Integration was started with horizontally averaged Levitus data. Interior relaxation to annual-mean Levitus temperature and salinity was continued for 3 years with a relaxation timescale of 1 year. This method of start-up avoids shocking the model with observed data that is incompatible with the model physics (Semtner and Chervin 1988). The model was then released from any interior relaxation and integrated for another 797 years. Two 800-year integrations were made in parallel—one of the unmodified model (control) and one of a model with relaxation to the maximum entropy equilibrium velocities (topographic stress). The models have not reached equilibrium after 800 years. Antarctic circumpolar transport is still increasing by 3% (5 Sv; Sar $\equiv 1 \times 10^6$ m^3 s^{-1}) and North Atlantic overturning is increasing by 0.5% (0.1 Sv), averaged over 100 years of integration. Although evolution continues, comparisons of trends can be made between parallel runs. Subsequent integrations have extended runs of a coarser-resolution model past 2000 years and qualitative differences between the control and topographic stress cases persist.

4. Results

Figure 1 shows the maximum entropy equilibrium velocities and depth-integrated transport as derived from (2) and (3). These velocities suggest currents that are opposite to many of the well-known surface currents such as the Gulf Stream, Canary, Brazil, and Benguela Currents or the Kuroshio, California, and Humboldt Currents. Magnitudes of statistical dynamical velocities are small, however, compared to the magnitude of the wind-driven surface currents, so we expect that topographic stress will have little effect on the large-scale surface circulation. At greater depths, where velocities from directly forced flows have smaller magnitude, topographic stress has relatively greater effect. One anticipates the development or strengthening of poleward undercurrents along eastern boundaries and equatorward undercurrents along western boundaries.

Velocities for the first few levels are similar for the parallel integrations since the surface circulation is dominated by wind and buoyancy forcing. After 800 years of integration, depth-integrated transports (Fig. 2) are broadly similar between the two cases since much of the transport is due to surface-intensified, directly forced flow. Although Fig. 2 and subsequent figures are instantaneous snapshots, the flow fields are quasi steady under annual mean forcing; hence flows may be considered time averaged over annual or multiannual timescales. Figure 2a is nearly a "textbook" figure, showing the main subtropical gyres and Antarctic Circumpolar Current. Defects such as weak western boundary recirculations and weak (or absent) subpolar gyres are not unexpected for coarse-resolution modeling.

With inclusion of topographic stress (Fig. 2b), differences are apparent even in this depth-integrated measure. Systematic differences appear in subpolar gyres (stronger in Fig. 2b) and in eastern boundary regimes, which are quiescent under conventional modeling but develop poleward flows under topographic stress, often reversing the sign of the circulation at subtropical latitudes. One observes also that the ap-

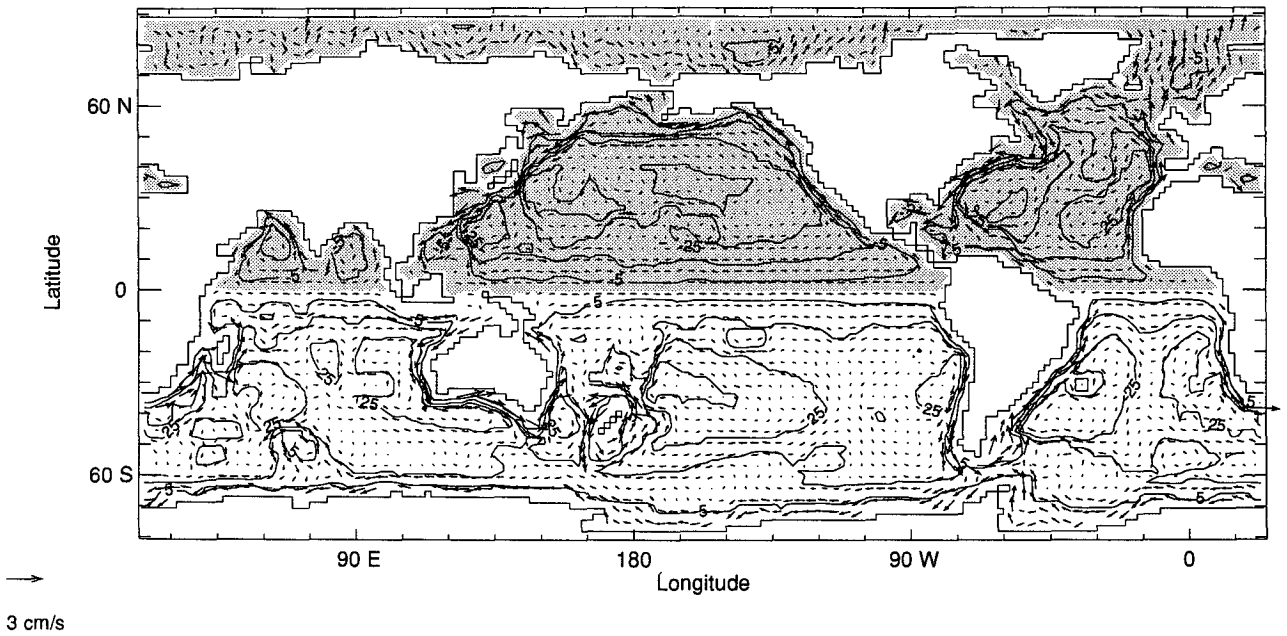

FIG. 1. (a) Maximum entropy equilibrium velocities and depth-integrated transport. Contour intervals are 10 Sv and stippling indicates negative values.

parent separations of western boundary currents (as inferred from transport streamfunction) are systematically shifted equatorward. Although transport streamfunction suggests an equatorward shift of the separations of western boundary currents, it also reflects the presence of stronger deep western boundary undercurrents. Peak transports in both the Gulf Stream and the Kuroshio are reduced [by 7 Sv (Sv $\equiv 10^6$ m^3 s^{-1})], in part due to stronger undercurrents. A host of other differences are seen such as the penetration of cyclonic circulation into the Labrador Sea.

What may be of immediate importance is only to observe that there are these many differences. The longer-term question will be to attempt to ascertain when a model development represents actual improvement in model fidelity. For the present we turn to more specific examination of velocity fields. Results from the model integrations will be discussed for two areas: the North Pacific and the Mid-Atlantic. The influence of topographic stress on the separation latitudes of western boundary currents and deep water exchange will also be discussed.

a. North Pacific velocities

Velocities at 405 m for the two integrations are shown in Fig. 3. Differences between the control run (Fig. 3a) and the topographic stress run (Fig. 3b) can be seen along the continental margins. The topographic stress run exhibits a California undercurrent, which is absent in the control, and a stronger Oyashio and Alaska Stream.

Observational evidence for an undercurrent along the west coast of North America is extensive, including work by Hickey (1979) off the coast of southern Washington, Freeland et al. (1984) off Vancouver Island, and Chelton (1984) off California. Measurements indicate poleward flow up to 15 cm s^{-1}, often with a width greater than 100 km, usually with a maximum at depths less than 700 m, but extending to more than 1000 m. Because most of these studies were coastal in nature, the width and depth of these undercurrents are not well observed: Actual widths of such flows may be too narrow to be resolved by coarse grids with spacings of order 100 km. However, property transports by narrow currents along continental margins may be significant, for example to nutrient budgets. The present calculation spreads boundary currents over the resolved grid spacing with speeds that reflect a compromise between swift narrow flows and a broader, presumably quieter offshore flow.

Although the generation of an undercurrent is encouraging, this may be a region where the parameterization has reduced overall model skill. One of the consequences of the relatively strong undercurrent is that the depth-integrated total transport of the California Current system is northward (Fig. 2b), while prevailing wisdom is that total transport should be southward.

Figure 4 shows velocities at 2880 m for both integrations. Coastal currents induced or strengthened by topographic stress at 405 m are seen more clearly at 2880 m, with a western boundary undercurrent now extending to the equator. There is a weak northward

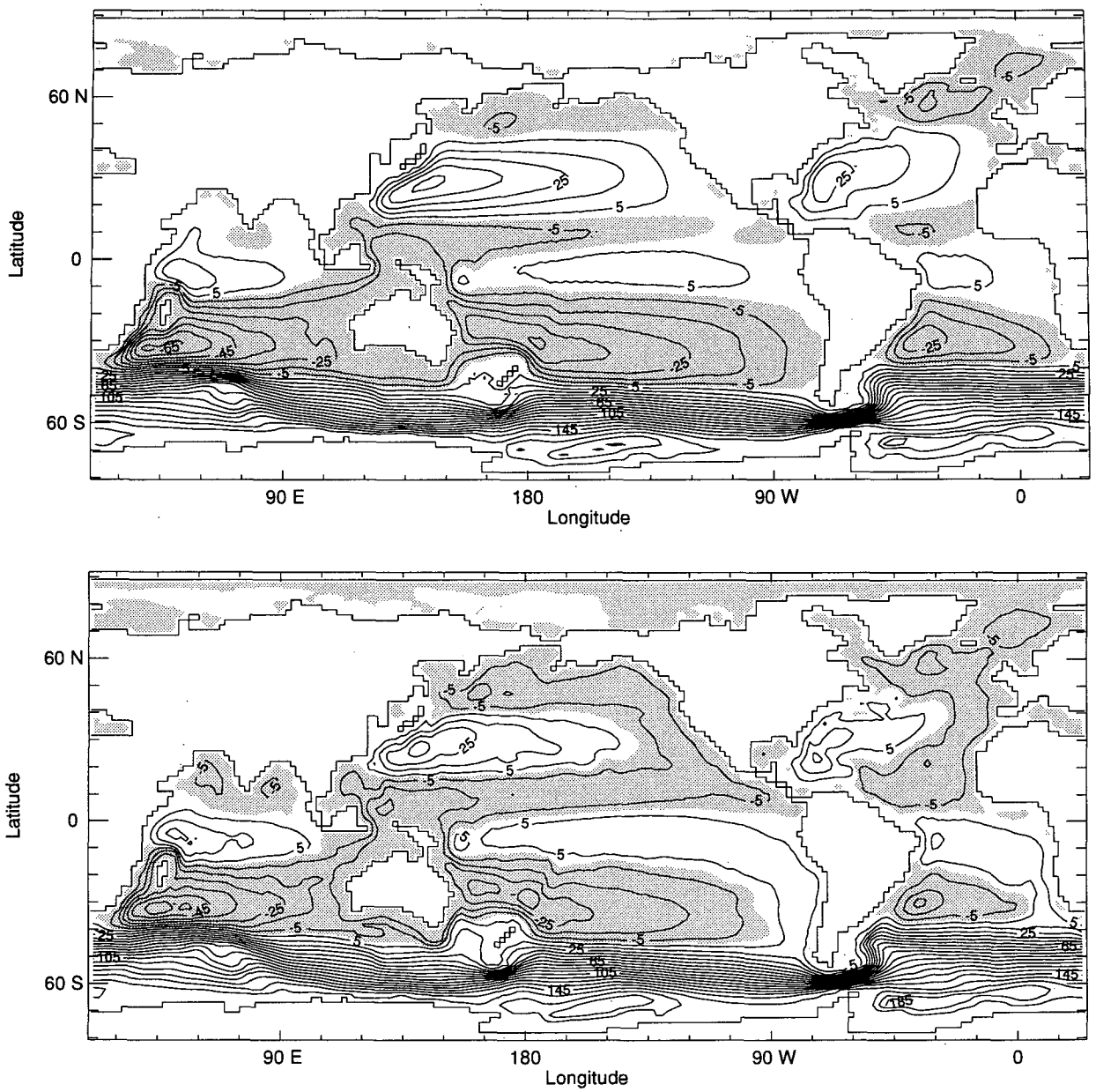

FIG. 2. Transport streamfunction for (a) the control case and (b) the topographic stress case. Contour intervals are 10 Sv and stippling indicates negative values.

current, opposing the inshore western boundary undercurrent, off of Japan.

Observations by Warren and Owens (1988) indicate a deep Alaska Stream flowing westward, with mean velocities between 1 and 3 cm s^{-1}, along the northern side of the Aleutian Trench. They also report evidence for a deep, eastward jet that flows parallel to the trench, south of the Alaska Stream. Direct observations of deep western boundary currents in the North Pacific are few. Indirect inference from tracers, such as silica (Talley and Joyce 1992), suggest northward deep flow along the western boundary. Current meter observations by Fukasawa et al. (1986) in the Shikoku Basin south of Japan (west of the region considered by Talley and Joyce 1992) show deep mean currents of 5 to 10 cm s^{-1} toward the southwest (parallel to local isobaths). Tracer evidence is consistent with a deep northward counterflow of low silica water, while the current meter observations support a deep, inshore, southward flowing boundary current.

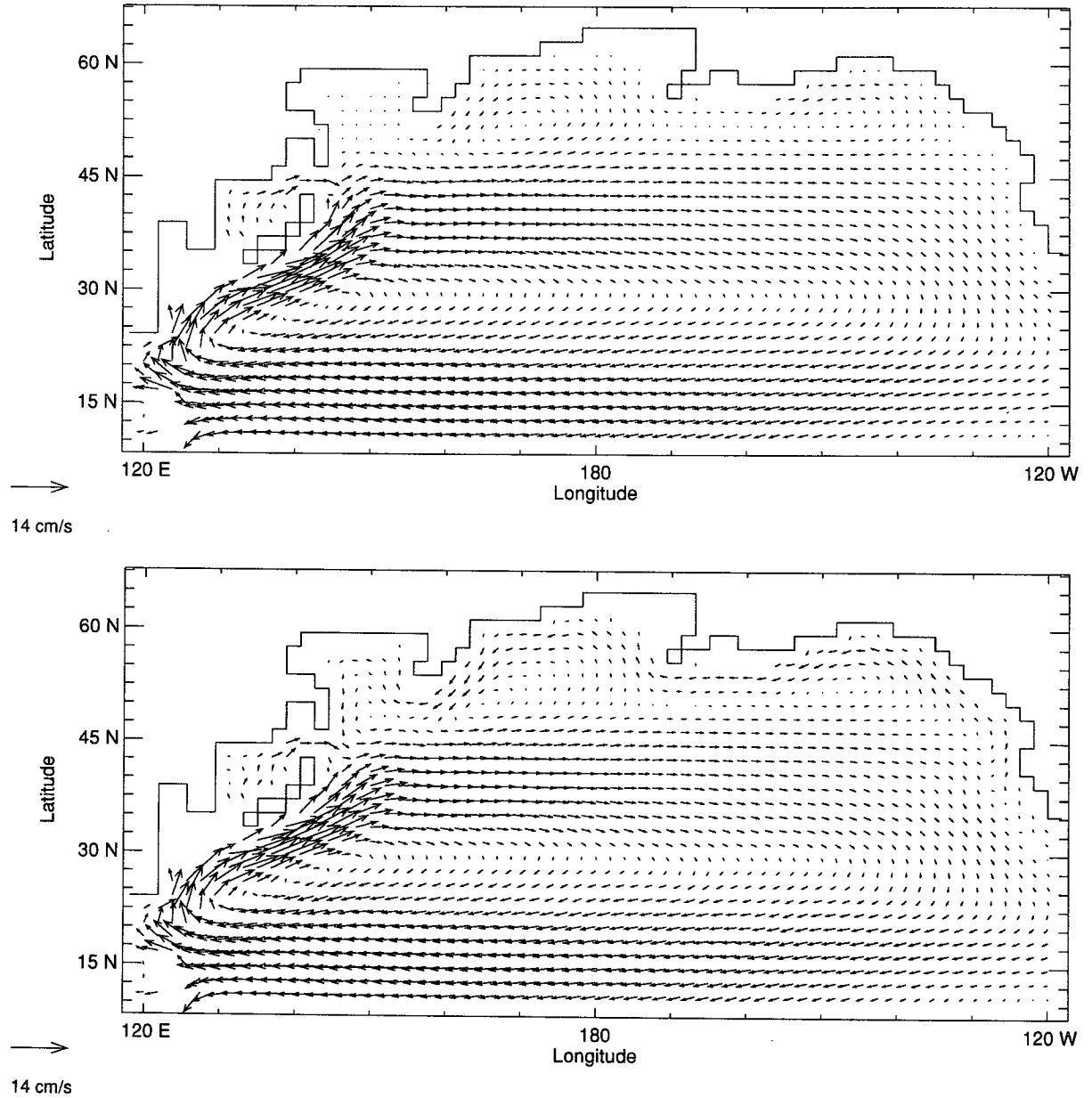

FIG. 3. Velocities at 405 m in the North Pacific for (a) the control case and (b) the topographic stress case.

The deep narrow trenches found in the Pacific are not resolved by this model, but could be important in setting up counterflows such as the one observed by Warren and Owens (1988) south of the Alaska Stream. At small scale the baroclinic influence should be taken into account; however, the barotropic formulation for topographic stress, (2) and (3), suggests a tendency for opposing currents on opposite sides of the trench, supporting northward and eastward transport of tracers in the deep western Pacific, while current meters on the inshore side of trenches show southward and westward flow.

b. Mid-Atlantic velocities

Model velocities at 845 m are shown in Fig. 5. Differences between the control run (Fig. 5a) and the topographic stress run (Fig. 5b) can be seen along the continental margins. Topographic stress has reversed the control run's equatorward eastern boundary currents and generated an inshore current counter to the Gulf Stream.

Poleward undercurrents have been observed off the west coast of South Africa (Nelson 1989) and off the coast of North Africa (Mittelstaedt 1989). Poleward

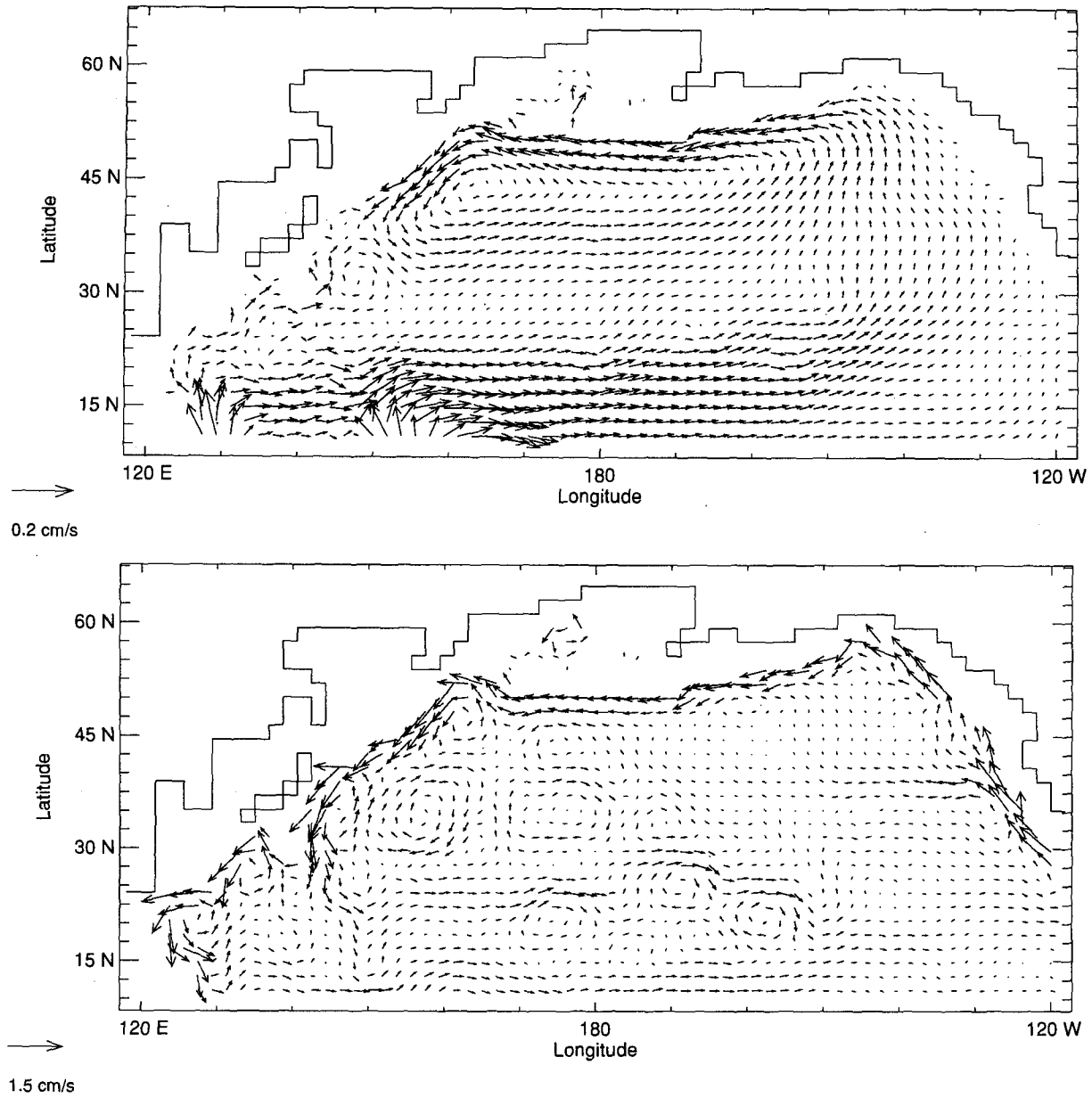

FIG. 4. As in Fig. 3 but at 2880 m. Note different velocity scales.

flow has also been described off the Iberian Peninsula (Barton 1989). Although spatial and temporal knowledge of poleward undercurrents along the eastern Atlantic is limited, direct measurements indicate a flow of up to 10 cm s^{-1} with a width of 30 to 100 km, usually with a maximum at about 300 m. The Peru–Chilean undercurrent is also present in Fig. 5b. This undercurrent has been seen from northern Peru to as far south as 41°S with speeds of 4–10 cm s^{-1} at depths of several hundred meters (Wooster and Gilmartain 1961).

Some of the strongest differences between the control and topographic stress runs occur along eastern margins where a tendency for poleward flow extends to great depth. Direct observations are few, suggesting opportunity to test some of the putative consequences of topographic stress, possibly contributing toward calibration of parameters such as L.

Figure 6 shows zonal velocity sections along 60°W in the North Atlantic. The topographic stress run (Fig. 6b) shows the core of the Gulf Stream at 39°N with westward flowing deep water hugging the coast underneath. This deep undercurrent is also seen moving eastward at 19° and 12°N. The control run (Fig. 6a) has the core of the Gulf Stream slightly north of 42° and develops a broader and weaker undercurrent.

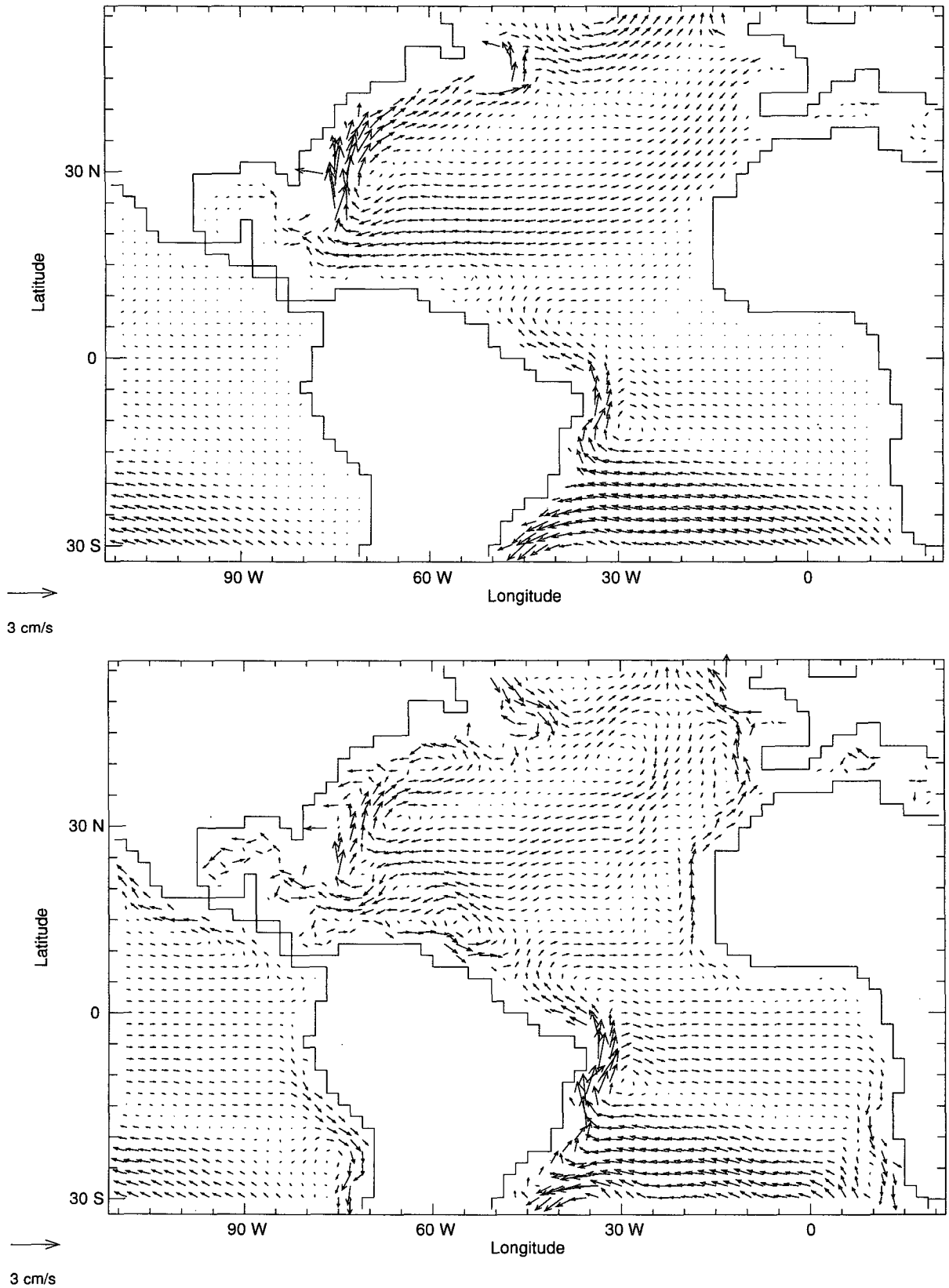

FIG. 5. As in Fig. 3 but at 845 m in the Mid-Atlantic.

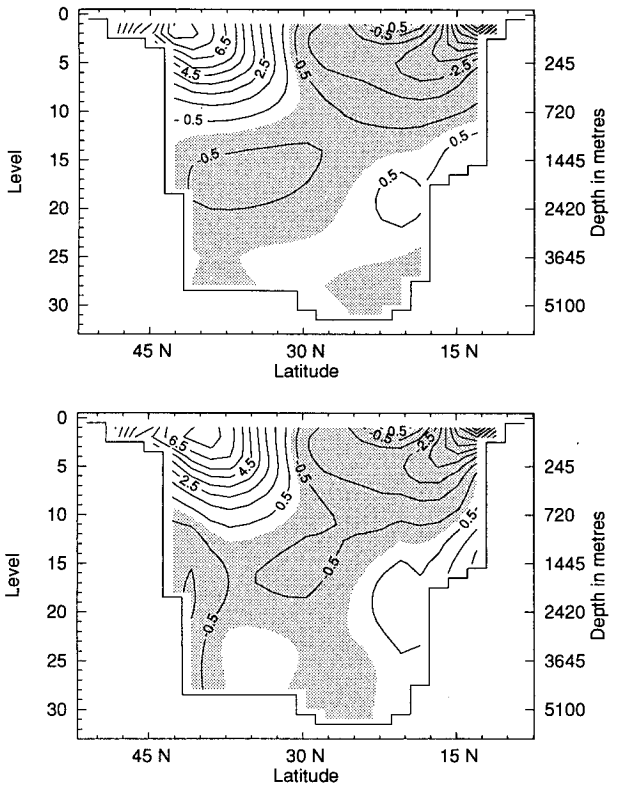

FIG. 6. Zonal velocity sections along 60°W in the North Atlantic for (a) the control case and (b) for the topographic stress case. Contour interval is 1 cm s^{-1} and stippling indicates westward flow.

Observations of the Gulf Stream at 60°W indicate a "north wall" path (determined by 15°C/200 m isotherm) that meanders between 42° and 37°N (Hansen 1970; Watts 1983). Observations of deep western boundary undercurrents in the North Atlantic show a strong core (up to 20 cm s^{-1}), within a few hundred kilometers of the coast, below 3000 m (Hogg 1983). The deep western boundary current observed off the Bahamas has similar characteristics, although the core appears to have ascended to about 2500 m (Lee et al. 1990).

c. *Implied surface heat flux*

Surface heat flux is calculated from the heat added (or lost) through relaxation to Levitus surface temperatures. The implied flux for the Kuroshio separation region can be seen in Fig. 7. Compared to the control (Fig. 7a), the topographic stress run (Fig. 7b) has a smaller maximum heat loss (by 30%) at a lower latitude. The absolute value of heat flux for these models is adjustable—in part it depends on the depth of the first layer, the vertical diffusion coefficient, and the relaxation timescale. Although it is difficult to compare the maximum values of heat loss to observations, the reduction and shift in the maximum does indicate a southward shift in the separation latitude of the Kuroshio. Reductions in the maximum implied freshwater flux are similar.

Equatorward shifts in separation latitude can also be seen for the Gulf Stream and Brazil Current (Figs. 2 and 6). Reductions in the maximum values of upward heat flux is about 18% near the separation of the Gulf Stream and 5% near the Brazil Current. Poleward overshoot of the separation latitude for western boundary currents is a common characteristic of both high- and low-resolution models (Bryan and Holland 1989; Cherniawsky and Holloway 1991; Haidvogel and Bryan 1992). Topographic stress appears to reduce or eliminate this overshoot.

d. *Deep-water formation and exchange*

Because the topographic stress parameterization (2) enters only the horizontal momentum equation, and because u^* is barotropic (for the coarse resolution in the present study), it is not clear that topographic stress should have much effect on quantities such as over-

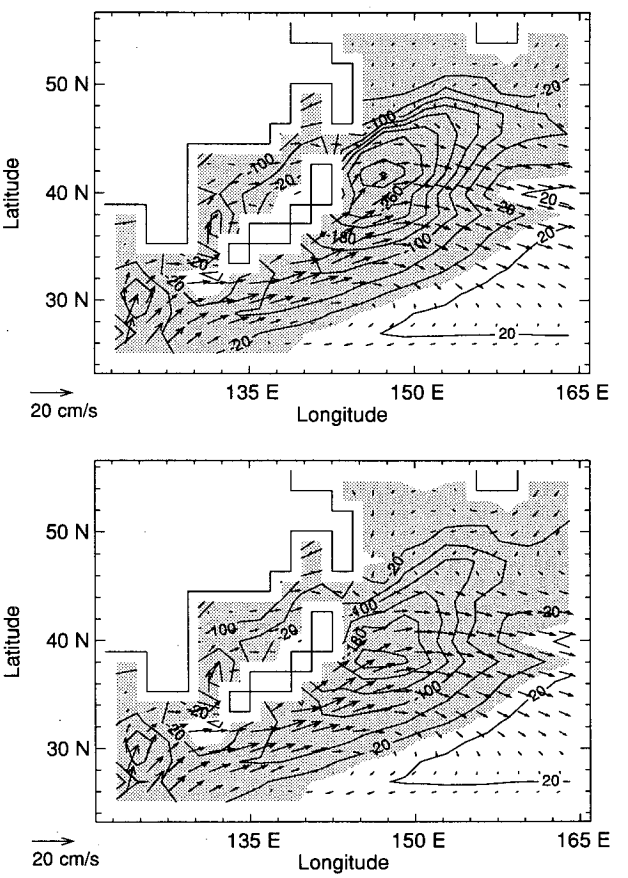

FIG. 7. Implied downward heat flux and surface velocities in the Kuroshio separation region for (a) the control case and (b) for the topographic stress case. Contour interval is 40 W m^{-2} and stippling indicates negative values.

turning streamfunction. In fact, the parameterization depends upon $u - u^*$, which has a depth dependence due to u. As well, by altering the horizontal flow, topographic stress alters the advection of density and hence may affect stability with respect to convection.

Figure 8a shows Atlantic overturning streamfunction from the control case. Familiar features include high-latitude sinking, subtropical convergence, and equatorial upwelling. Although the model is not yet in equilibrium, strengths of the cells, especially the northern sinking, are less than what is thought to be realistic. At the coarse resolution of the model, and given the simple boundary conditions, the weakness of circulation might be expected. As Maier-Reimer et al. (1993) remark, surface forcing conditions are uncertain. By altering the forcing (buoyancy loss) at high latitudes, one may induce more or less sinking. Yet, with annual mean heat loss exceeding 200 W m^{-2} (winter values exceeding 300 W m^{-2}) over the East Greenland Current, Maier-Reimer et al. note that their model fails to produce sufficient North Atlantic Deep Water. Toggweiler et al. (1989) also find that their model does not remove enough deep water from the North Atlantic to agree with observations.

Figure 8b shows the difference in Atlantic overturning streamfunction between the topographic stress case and the control case, that is, the change in overturning attributable to topographic stress. Although there is a slight shallowing of deep-water formation, interhemispheric exchange is stronger (by about 20%) with southward transport in middepths and increased northward transport at abyssal depths. It is premature to suggest that Fig. 8b indicates an improvement in model skill. Care should be exercised when interpreting overturning streamfunction, as with transport streamfunction. Topographic stress acts to increase the gyre component of circulation, as deep equatorward transports along western boundaries are substantially compensated by poleward undercurrents along eastern boundaries. The parameterization enhances deep water exchange to even a greater degree than would be supposed from differences in overturning streamfunction.

For the present we only observe that there are differences in Fig. 8b. A familiar description of the ocean circulation is the global conveyor belt (Gordon 1986; Broecker 1987), forced by high-latitude sinking. Figures 1 and 8b suggest the conveyor belt could be in part driven by topographic stress, implying a more persistent ocean circulation despite climate-induced changes in high-latitude sinking.

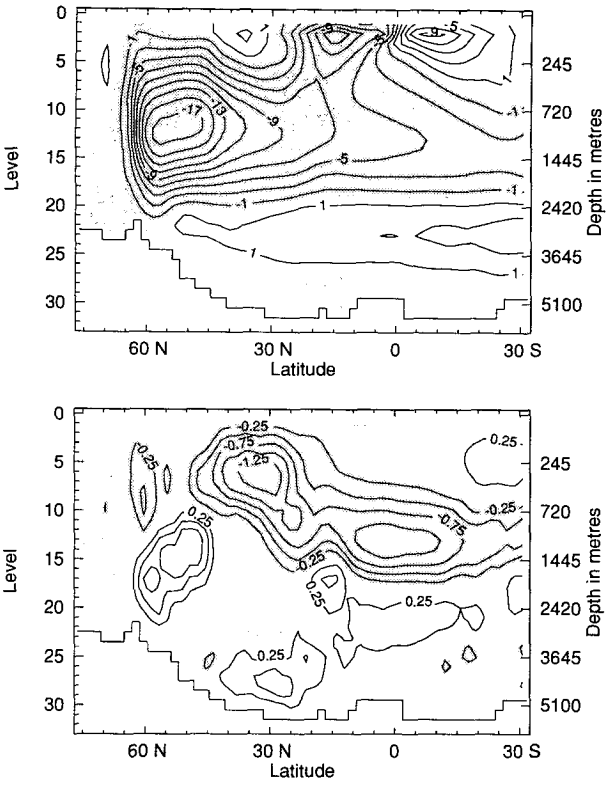

FIG. 8. North Atlantic overturning streamfunction for (a) the control case and (b) for the difference between the topographic stress and control case. Contour intervals are 2 Sv and 0.25 Sv, respectively, and stippling indicates counterclockwise circulation.

5. Applicability

Longer runs were carried out at coarser resolution in order to assess the generality and longer-term response of the parameterization. A global model was created with twice the vertical and horizontal grid spacing (3.711° by 3.75° by 15 levels and five islands), horizontal viscosity and diffusivity were increased by 2.5 times and the time step doubled. All other parameters were the same as for the finer-resolution model. Two 2000-year integrations were made in parallel—one of the unmodified model and one of a model with relaxation to the maximum entropy equilibrium velocities.

The difference in transport streamfunction (topographic stress minus control), after 800 years of integration, for the finer-resolution model is shown in Fig. 9a and for the coarser-resolution model in Fig. 9b. These figures show similar responses, indicating that, at least for depth-integrated transport, resolution has relatively little effect on the model's response to the parameterization. Perhaps the most obvious difference (enhanced by stippling) is that total Antarctic Circumpolar Current transport is decreased by the parameterization in the fine-resolution model and increased in the coarse-resolution model. However, given the great sensitivity of the transport to resolution, approximately 160 Sv in the fine-resolution and 80 Sv in the coarse-resolution cases, small differences in the response might be expected. In both cases, the main effect of topographic stress in this area is to provide a westward difference in transport of several Sverdrups along

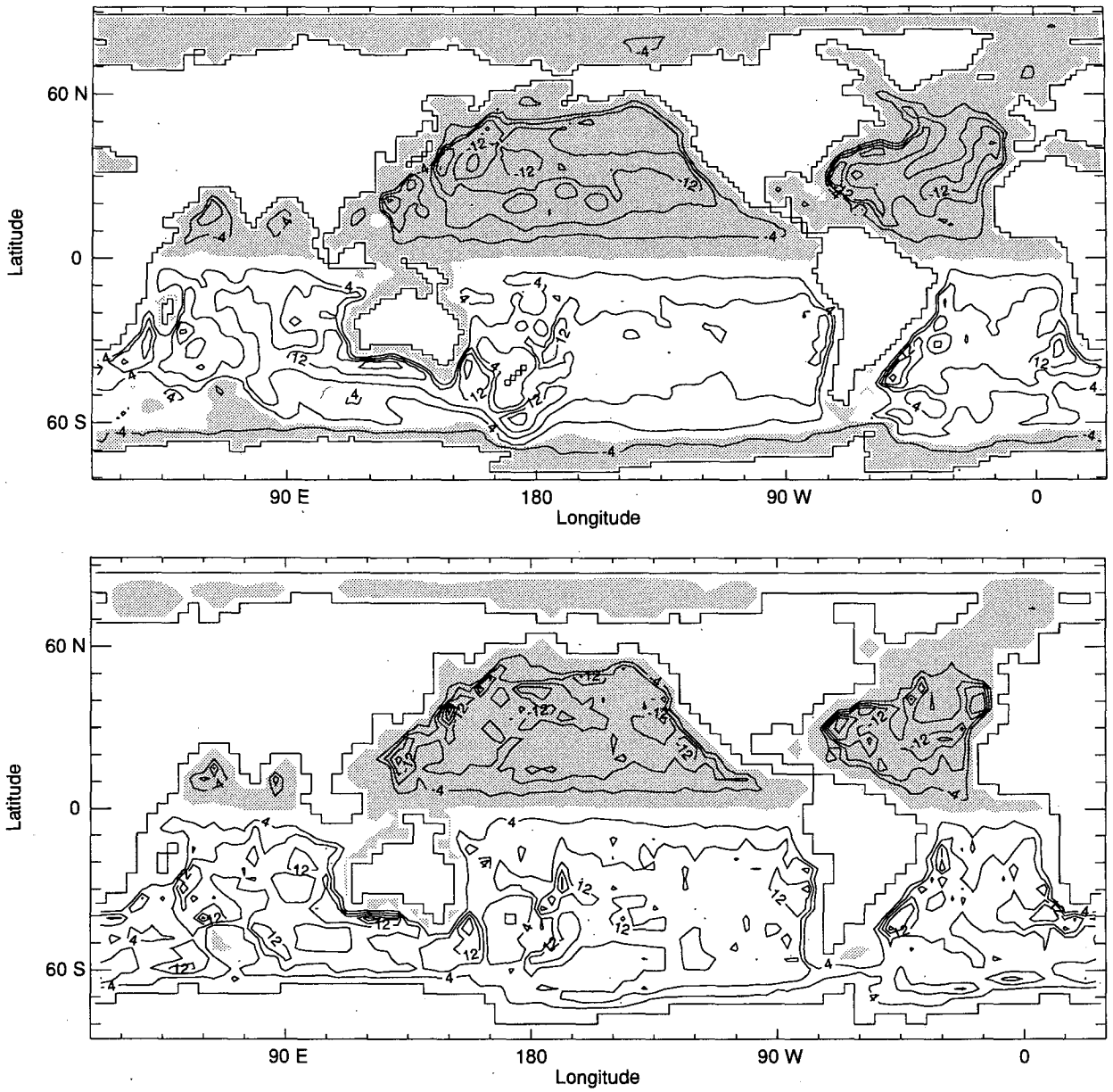

FIG. 9. Transport streamfunction difference (topographic stress case minus control case) for (a) the 1.8° model and (b) the 3.7° model. Contour intervals are 4 Sv and stippling indicates negative values.

the Antarctic margin. The response of the coarse-resolution model after 2000 years (not shown) is almost identical to the response after 800 years with minor differences confined to the still evolving Antarctic Circumpolar Current.

With similar differences in transport, induced boundary currents in the low-resolution model are generally more spread out and have lower peak velocities than in the higher-resolution model. Thus, the detail and local response of the model is affected by resolution. These runs also indicate that the value chosen for L is relatively insensitive to resolution. For areas where the deformation radius differs from the global average, L may have to be adjusted. Studies by Alvarez et al. (1994) in the Mediterranean showed that an appropriate value of L is approximately half of the latitude-dependent value used in this study. A refinement to the parameterization presented here could consist of making L proportional to the regionally averaged deformation radius.

Outstanding issues include the physical basis for estimation of L, and the appropriateness of using the $A_m\nabla^2$ operator as a means for incorporating topographic stress. For our present study we have considered

only annual-mean forcing; greater realism would take account of seasonality. The parameterization reflects the length scale of eddies (not their energetics) and should not have to be altered under seasonal or interannual forcing. If the parameterization is extended to finer resolution, there will be at least two further considerations. When the first radius of deformation is sufficiently resolved, the maximum entropy configuration for smaller-scale mean flow features will become bottom trapped. As well, when flows become eddy active and the eddies are sufficiently well resolved, then realization of entropy-increasing tendency will be realized explicitly by the resolved eddies. Addressing these questions will require substantial effort over time.

6. Summary

The GFDL Modular Ocean Model was used to explore a representation of topographic stress. The most apparent effects of topographic stress are seen along continental margins, particularly in the development or strengthening of undercurrents. Integrations that include topographic stress produce many of the observed poleward eastern boundary undercurrents whereas the control run does not. Along western boundaries, topographic stress produces narrow equatorward undercurrents, often with an offshore countercurrent. Topographic stress reduces the overshoot of the separation latitudes for western boundary currents and contributes to deep water exchange.

Considering the many aspects of model output that are altered by inclusion of topographic stress (for the given choices of parameters), it seems clear that this effect may be significant. There is also the suggestion that model output may be "improved" in various regards in diverse regions. A danger certainly is the appearance of right answers for wrong reasons. Given the many uncertainties of ocean models (uncertain forcing functions, different numerical formulations, sundry tuneable parameters) the inference of "right reasons" is hazardous. The present study has demonstrated model sensitivity to a suggested parameterization of topographic stress. We hope this better motivates fresh research to bridge some of the gaps between ideal quasigeostrophic statistical dynamics and the full physics of forced–dissipative oceans.

Acknowledgments. Critical suggestions from anonymous reviewers have helped guide revisions to this paper. This work was carried out with the support of the Office of Naval Research Grants N00014-87-J-1262 and N00014-92-J-1775.

REFERENCES

Alvarez, A., J. Tintore, G. Holloway, M. Eby, and J. M. Beckers, 1994: Effect of topographic stress on the circulation in the western Mediterranean. *J. Geophys. Res.*, **99,** 16 053–16 064.

Barton, E. D., 1989: The poleward undercurrent of the eastern boundary of the subtropical North Atlantic. *Poleward Flows Along Eastern Ocean Boundaries,* S. J. Neshyba, C. N. K. Mooers, R. L. Smith, and R. T. Barber., Eds., Springer-Verlag, 82–95.

Broecker, W. S., 1987: The biggest chill. *Nat. Hist.* **97,** 74–82.

Bryan, F., and W. R. Holland, 1989: A high resolution simulation of the wind- and thermohaline-driven circulation in the north Atlantic ocean. *'Aha Huliko'a Parameterization of Small-Scale Processes,* P. Muller and D. Henderson, Eds., Hawaii Institute of Geophysics, 99–116.

Bryan, K., 1969: A numerical method for the study of the circulation of the World Ocean. *J. Comput. Phys.*, **4,** 347–376.

——, 1984: Accelerating the convergence to equilibrium of ocean–climate models. *J. Phys. Oceanogr.*, **14,** 666–673.

Chelton, D. B., 1984: Seasonal variability of alongshore geostrophic velocity off central California. *J. Phys. Oceanogr.*, **12,** 757–784.

Cherniawsky, J., and G. Holloway, 1991: An upper-ocean general circulation model for the North Pacific: Preliminary experiments. *Atmos.–Ocean,* **29,** 737–784.

Cox, M. D., 1984: A primitive equation, three-dimensional model of the ocean. GFDL Ocean Group Tech. Rep. No. 1. [Available from Geophysical Fluid Dynamics Laboratory, NOAA, Princeton University, Princeton, NJ 08542.]

Cummins, P., and G. Holloway, 1994: On eddy–topographic stress representation. *J. Phys. Oceanogr.*, **24,** 700–706.

ETOPO5, 1986: Global 5′ × 5′ depth and elevation. [Available from National Geophysical Data Center, NOAA, U.S. Dept. of Commerce, Code E/GC3, Boulder, CO 80303.]

Freeland, H. J., W. R. Crawford, and R. E. Thompson, 1984: Currents along the Pacific coast of Canada. *Atmos.–Ocean,* **22,** 151–172.

Fukasawa, M., T. Teramoto, and K. Taira, 1986: Abyssal current along the northern periphery of Shikoku Basin. *J. Oceanogr. Soc. Japan,* **42,** 459–472.

Gordon, A. L., 1986: Interocean exchange of thermocline water. *J. Geophys. Res.*, **91,** 5037–5046.

Haidvogel, D. B., and F. O. Bryan, 1992: Ocean circulation modeling. *Climate System Modeling,* K. E. Trenberth, Ed., Cambridge University Press, 371–412.

Hansen, D. V., 1970: Gulf Stream meanders between Cape Hatteras and the Grand Banks. *Deep-Sea Res.*, **17,** 495–511.

Hellerman, S., and M. Rosenstein, 1983: Normal monthly wind stress over the World Ocean with error estimates. *J. Phys. Oceanogr.*, **13,** 1093–1104.

Hickey, B. M., 1979: The California Current System—hypotheses and facts. *Progress in Oceanography,* Vol. 8, Pergamon, 191–279.

Hogg, N. G., 1983: A note on the deep circulation of the western North Atlantic: Its nature and causes. *Deep-Sea Res.*, **30,** 945–961.

Holloway, G., 1992: Representing topographic stress for large-scale ocean models. *J. Phys. Oceanogr.*, **22,** 1033–1046.

Lee, T. N., W. Johns, F. Schott, and R. Zantopp, 1990: Western boundary current structure and variability east of Abaco, Bahamas, at 26.5°N. *J. Phys. Oceanogr.*, **20,** 446–466.

Levitus, S., 1982: *Climatological Atlas of the World Ocean.* NOAA Prof. Paper No. 13, Washington, D.C., 173 pp.

Maier-Reimer, E., U. Mikolajewicz, and K. Hasselmann, 1993: Mean circulation of the Hamburg LSG OGCM and its sensitivity to the thermohaline surface forcing. *J. Phys. Oceanogr.*, **23,** 731–757.

Mittelstaedt, E., 1989: The subsurface circulation along the Moroccan slope. *Poleward Flows Along Eastern Ocean Boundaries,* S. J. Neshyba, C. N. K. Mooers, R. L. Smith, and R. T. Barber, Eds., Springer-Verlag, 96–109.

Nelson, G., 1989: Poleward motion in the Benguela area. *Poleward Flows Along Eastern Ocean Boundaries,* S. J. Neshyba, C. N. K. Mooers, R. L. Smith, and R. T. Barber, Eds., Springer-Verlag.

Pacanowski, R., K. Dixon, and A. Rosati, 1991: The G.F.D.L. Modular Ocean Model users guide version 1.0. GFDL Ocean Group Tech. Rep. No. 2. [Available from Geophysical Fluid Dynamics Laboratory, NOAA, Princeton University, Princeton, NJ 08542.]

Salmon, R., G. Holloway, and M. C. Hendershott, 1976: The equilibrium statistical mechanics of simple quasi-geostrophic models. *J. Fluid Mech.*, **75,** 375–386.

Semtner, A. J., 1974: A general circulation model for the World Ocean. UCLA Dept. of Meteor. Tech. Rep. No. 8, 99 pp.

——, and R. M. Chervin, 1988: A simulation of the global ocean circulation with resolved eddies. *J. Geophys. Res.*, **93,** 15 502–15 522.

Talley, L. D., and T. M. Joyce, 1992: The double silica maximum in the North Pacific. *J. Geophys. Res.*, **97,** 5465–5480.

Toggweiler, J. R., K. Dixon, and K. Bryan, 1989: Simulations of radiocarbon in a coarse-resolution world ocean model 1. Steady state prebomb distributions. *J. Geophys. Res.*, **94,** 8217–8242.

Warren, B. A., and W. B. Owens, 1988: Deep currents of the central subarctic Pacific Ocean. *J. Phys. Oceanogr.*, **18,** 529–551.

Watts, D. R., 1983: Gulf stream variability. *Eddies in Marine Science,* A. R. Robinson, Ed., Springer-Verlag, 114–144.

Wooster, W. S., and M. Gilmartain, 1961: The Peru–Chile undercurrent. *J. Mar. Res.*, **19,** 97–122.